Deposition of germanium dioxide films by the injection of oxygen ion beam in conjunction with hexamethyldigermane

Satoru Yoshimura[a*], Satoshi Sugimoto[a], Takae Takeuchi[a],

Kensuke Murai[b], and Masato Kiuchi[a,c]

[a]Division of materials and manufacturing science, Graduate School of Engineering, Osaka University, Suita, Osaka 565-0871, Japan.

[b] National Institute of Advanced Industrial Science and Technology (AIST), Ikeda, Osaka 563-8577, Japan.

[c] Cerast Laboratory, Setagaya, Tokyo 154-0011, Japan.

*corresponding author

E-mail: yosimura@ppl.eng.osaka-u.ac.jp (Satoru Yoshimura)

HIGHLIGHTS

- Germanium dioxide films have attracted much attention to its practical applications.
- A methodology for fabricating germanium dioxide films was presented.
- We used hexamethyldigermane (HMDG) as a source material.
- Germanium dioxide films were formed when O^+ ions were irradiated in conjunction with HMDG.

Keywords:

ion beam induced deposition;

germanium dioxide;

oxygen ion beam;

hexamethyldigermane

ABSTRACT

We proposed a methodology for fabricating a film by the simultaneous injections of O^+ ions and hexamethyldigermane (HMDG) to a substrate. The O^+-ion energy was set at 50 eV. After the experimental trial, we found a film deposited on the substrate. The analyses of the film with X-ray photoelectron spectroscopy and Fourier transform infrared spectroscopy showed that the deposited film was germanium dioxide (GeO_2). It was also noted that no film deposition occurred when HMDG was supplied to substrates without O^+-ion beam injections. In conclusion, the low-energy O^+-ion beam induced deposition using HMDG was found to be useful for the deposition of GeO_2 films.

1. Introduction

The ion-beam-induced chemical vapor deposition (IBICVD) method is useful for fabricating nanometer-scale 3D structures [1] and ferromagnetic materials [2]. It can also be used to prepare films of metal oxides such as TiO_2 [3, 4], Al_2O_3 [4], ZrO_2 [5], and SiO_2 [6-9]. The IBICVD method enables films to be deposited at the exact location where both the source material and ion beam contact the substrate.

Germanium oxide films have attracted much attention because of their suitability for use in practical applications such as optical waveguides [10], semiconductors [11], passivation layers [12], rutile substrates [13], and optical memory devices [14]. Germanium oxide films can be produced via various methods such as radio-frequency sputtering [15-18], vacuum evaporation [19], atomic-layer deposition [20], thermal oxidation [21], anodic oxidation [22], ozone oxidation [23], and plasma oxidation [24].

Although IBICVD is a powerful tool for producing metal oxide films [3-9], the literature contains no reports concerning its use for the fabrication of germanium oxide films. In most cases, germanium oxide films formed by the aforementioned methods [15-24] were

deposited uniformly over the substrates. By contrast, films deposited by the IBICVD method can, in principle, be deposited at the exact location where both the source material and ion beam contact the substrate.

For the production of germanium oxide films by IBICVD, a suitable source material must first be selected. Hexamethyldigermane [HMDG, $(CH_3)_3GeGe(CH_3)_3$] is a molecular substance that contains two Ge atoms per molecule. We therefore selected HMDG as a source material for IBICVD. In addition, we selected an O^+-ion beam. In the present study, O^+-ion beams with various energies were used to irradiate a substrate, in conjunction with a flow of HMDG. After the experiments, we observed films deposited on the substrates. The deposited films were subsequently analyzed by X-ray photoelectron spectroscopy (XPS), X-ray diffraction (XRD), X-ray reflectometry (XRR), and Fourier-transform infrared (FTIR) spectroscopy.

2. Materials and Method

The film formation trials were carried out using an ion-beam injection system. A schematic view of the system is provided elsewhere [25]. In the present study, pure carbon

dioxide (CO_2) gas was used for O^+-ion production. Specifically, O^+ ions were produced by the decomposition of CO_2 gas in a Freeman-type ion source of the beam system and were then extracted. After mass-selection, the O^+ ions were guided to the processing chamber of the beam system, where they irradiated a substrate at normal incidence.

A schematic of the process chamber is shown in Fig. 1. The base pressure in the chamber was 1×10^{-6} Pa. Liquid HMDG (Sigma-Aldrich Co. LLC) in a stainless steel container was used as a source material. The HMDG vapor was extracted from the container using Ar as a carrier gas. The mixed gas (HMDG + Ar) was supplied to the substrate surface at 0.7 sccm, in conjunction with the incident O^+-ion beam. The pressure was 1×10^{-3} Pa during the trial.

An Au-coated quartz crystal microbalance (QCM) substrate (ULVAC, CRTS-0) or an untreated Si substrate (15 × 15 mm) was used as a substrate for O^+-ion beam irradiation. The diameter of the film deposition area on the QCM substrate was 7.5 mm. Both substrates were used at room temperature. The change in the mass of the film deposited on the QCM substrate was measured using a QCM controller (ULVAC, CRTM-9000). After the experimental trials, the deposited films were analyzed by XPS (ULVAC-PHI,

ESCA-3057), stylus profilometry (KLA-Tencor, P-15), XRD (RIGAKU, RINT2200), XRR (RIGAKU, Smart Lab), and FTIR spectroscopy (Jasco, FT/IR-410).

3. Results and discussion

Prior to the film formation experiments, the mass of the incident ions was measured using a mass and energy analyzer (barzers, PPM-421), and the results are shown in Fig. 2. The mass of the incident ions was 16 u (Fig. 2). Therefore, the incident ions were O^+ ions without impurity ions. The results of ion-energy measurements using the PPM-421 analyzer show that the peak energy in the ion energy distribution was 50 eV (Fig. 3). The profile of the ion beam was also acquired (Fig. 4).

During experiments to form germanium oxide films via O^+-ion beam irradiation of Si substrates in the presence of HMDG, we could not determine whether a film was actually formed on the substrate surface unless we removed the substrate from the process chamber and analyzed its surface using an instrument such as a stylus profiler. Therefore, in the first trial, we irradiated a QCM substrate with an O^+-ion beam in the presence of HMDG. We could then recognize that a film was formed without removing the substrate

114 from the process chamber. The mass of the deposited film was measured *in situ* using the
115 CRTM-9000 controller.
116
117 Before the IBICVD trial, we irradiated the QCM substrate with an O^+-ion beam without
118 supplying HMDG, and found that no film was deposited. Trials in which HMDG was
119 supplied to the substrate without O^+-ion irradiation also showed no film deposition.
120
121 The QCM substrate was subsequently irradiated with O^+-ion beams of various energy
122 while HMDG was supplied to the substrate. We performed five trials in which the peak
123 O^+ energy was 20, 50, 75, 100, or 200 eV, corresponding to current densities of 0.5, 1.3,
124 1.6, 1.4, and 1.1 $\mu A/cm^2$, respectively. After each trial, a film was found to have been
125 deposited onto the substrate. The masses of the deposited films were measured using the
126 CRTM-9000 controller, and the results are shown in Fig. 5. We found that the film mass
127 in the 50 eV case was greater than those in the 20, 75, 100, and 200 eV cases. Therefore,
128 subsequent film formation experiments were carried out using a 50 eV O^+-ion beam.
129
130 We irradiated a QCM substrate with a 50 eV O^+-ion beam while supplying HMDG to the
131 substrate. The duration of the ion-beam injection was 800 min. After the trial, we analyzed
132 the deposited film using the CRTM-9000 controller, revealing the film mass to be 5 μg.

The deposited film was further analyzed by XPS using an ESCA-3057 X-ray photoelectron spectrometer equipped with an Al K_α radiation source. In the present study, the operating parameters for the ESCA-3057 spectrometer were an energy step of 0.2 eV and a dwell time of 20 ms; the number of scans per spectrum was 10. Energy calibration of the ESCA-3057 spectrometer was regularly performed using standard reference specimens. The acquired XPS spectra are shown in Fig. 6. The binding energies in the Ge3*d* [Fig. 6(a)] and O1*s* [Fig. 6(b)] spectra indicate that the deposited film was germanium oxide. The O/Ge atomic ratio calculated from the XPS data was 2 (i.e., GeO_2). The C1*s* XPS spectrum [Fig. 6(c)] of the film shows that no carbon atoms were included in the film.

We next attempted to obtain an FTIR spectrum of the deposited film. However, the film deposited on the QCM substrate was not suitable for FTIR analysis because infrared radiation did not penetrate the substrate. Therefore, to obtain a film suitable for FTIR analysis, a 50 eV O^+-ion beam was used to irradiate a Si substrate in the presence of HMDG. The experimental parameters were the same as those in the experiments using the QCM substrates. The duration of ion-beam irradiation was 2950 min. After the IBICVD experiment, we found that a film had formed on the Si substrate.

We first measured the thickness of the film using a stylus profiler. The measurement showed that the film was ~100 nm thick.

The FTIR spectrum of the film (Fig. 7) was obtained using an FT/IR-410 spectrometer in transmission mode with subtraction of the contribution of the Si substrate. The bands at ~2350 cm^{-1} in the FTIR spectrum are attributed to CO_2 gas remaining inside the measurement chamber of the spectrometer. The strong peak observed at ~900 cm^{-1} is known to correspond to GeO_2 [26].

The deposited film on the Si substrate was analyzed by XRR. XRR measurements of the film showed that the thickness, density, and roughness of the film were 101 nm, 3.9 g/cm^3, and 11 nm, respectively.

The deposited film on the Si substrate was subsequently analyzed by XRD using an RINT2200 X-ray diffractometer. The wavelength of the X-rays was λ = 1.78892 Å (Co $K_{\alpha 1}$), and the X-ray beam was incident to the film surface at an angle θ. The obtained XRD pattern (θ-2θ method) shows no obvious peaks (Fig. 8), suggesting that no crystalline structures were present in the film.

Matsutani et al. pioneered the IBICVD method using HMDG as a source material [27]. In their experiments, a Si substrate was irradiated with an Ar^+-ion beam while HMDG

was simultaneously supplied to the substrate. They reported the deposition of amorphous germanium carbide (GeC) films. No experiments have been reported concerning the simultaneous use of an O^+-ion beam and HMDG, as conducted in the present study. Irrespective of the variety of available experimental methods, no previous experiments using HMDG as a source material for GeO_2 film deposition have been reported.

Yoshimura et al. attempted to use HMDG as a source material in a low-energy molecular-ion-beam deposition method and proposed a method for fabricating amorphous GeC films by injecting $GeCH_x$ molecular ions produced by the decomposition of HMDG into substrates [28]. They reported that amorphous GeC films were formed only when the $GeCH_x$ ion energy was less than 30 eV. They also found that, when $GeCH_x$ ions were injected into substrates with an energy of 30 eV or more, the bonds between Ge and C in the $GeCH_x$ ions were broken and Ge and C failed to recombine on the substrate. By contrast, we found that, when O^+-ion beams were used to irradiate a substrate while HMDG was simultaneously sprayed onto the substrate, the bonds between Ge and C in the HMDG molecules were broken and then Ge atoms combined with O atoms to form GeO_2 films on the substrate.

Sigma-Aldrich Co. LLC produces a very small quantity of HMDG and sells it only for research purposes. For this reason, only a few groups have reported studies related to HMDG, such as electron spin resonance measurements [29], identification of fragment ions [30, 31], and chemical applications [32]. HMDG has attracted little attention; thus, little interest has been expressed in its industrial applications. There have been no attempts thus far to apply HMDG in industrial fields. HMDG is an expensive reagent

(~$100 USD per gram). Because our proposed method uses HMDG as a source material, the current methodology is more expensive than other reported germanium oxide film-forming methods [15-24]. However, we emphasize that, if applications of HMDG (e.g., the GeO_2 deposition method proposed in the present study) become widespread in industrial and technological fields, chemical companies such as Sigma-Aldrich Co. LLC might produce and sell HMDG in larger quantities, drastically reducing its cost.

4. Conclusion

An experimental methodology for GeO_2 film formations using HMDG as a source material was presented. HMDG was supplied onto the substrate surface together with the O^+-ion beam. The O^+-ion energy was 50 eV. The substrate was set at room temperature. We found a film formed on the substrate after the trial. The XPS and FTIR results showed that the film was GeO_2. In addition, the film mass obtained at five different O^+ energy levels (20, 50, 75, 100, and 200 eV) was evaluated. The mass of the deposited film obtained following 50 eV injection was larger than those obtained following 20, 75, 100, and 200 eV injections. In conclusion, the 50 eV O^+-ion beam induced deposition using HMDG was found to be useful for the formation of the GeO_2 film.

Acknowledgments

The authors wish to thank Professor S. Hamaguchi (Osaka University) for valuable suggestions. The authors thank FORTE Science Communications (https://www.forte-science.co.jp/) for English language editing.

Declaration

Author Contributions

Satoru Yoshimura: Conceived and designed the experiments; Performed the experiments; Wrote the paper.

Satoshi Sugimoto: Performed the experiments; Contributed reagents, materials, analysis tools or data.

Takae Takeuchi: Analyzed and interpreted the data; Contributed reagents, materials, analysis tools or data.

Kensuke Murai: Performed the experiments; Contributed reagents, materials, analysis tools or data.

Masato Kiuchi: Analyzed and interpreted the data; Contributed reagents, materials, analysis tools or data.

Funding statement

This research did not receive any specific grant from funding agencies in the public, commercial, or not-for-profit sectors.

Data Availability Statement

Data will be made available on request.

Declaration of interest's statement

The authors declare no conflict of interest.

Additional information

No additional information is available for this paper.

References

[1] S. Matsui, Focused-ion-beam deposition for 3-D nanostructure fabrication, Nucl. Instrum. Method Phys. Res. B 257 (2007) 758-764.

[2] Q. Y. Xu, Y. Kageyama, T. Suzuki, Ion-beam-induced chemical-vapor deposition of FePt and CoPt particles, J. Appl. Phys. 97 (2005) 10K308.

[3] D. Leinen, A. Fernandez, J. P. Espinos, T. R. Belderrain, A. R. Gonzalez-Elipe, Ion beam induced chemical vapor deposition for the preparation of thin film oxides, Thin Solid Films 241 (1994) 198-201.

[4] D. Leinen, A. Fernandez, J. P. Espinos, A. R. Gonzalez-Elipe, Preparation of TiO_2 and Al_2O_3 thin films by ion-beam induced chemical vapor deposition, Vacuum 45 (1994) 1043-1045.

[5] J. P. Holgado, M. Perez-Sanchez, F. Yubero, J. P. Espinos, A. R. Gonzalez-Elipe, Corrosion resistant ZrO_2 thin films prepared at room temperature by ion beam induced chemical vapor deposition, Surf. Coat. Technol. 151-152 (2002) 449-453.

[6] S. Yoshimura, S. Sugimoto, T. Takeuchi, M. Kiuchi, Low-energy O^+ ion beam induced chemical vapor deposition using hexamethyldisilane or hexamethyldisilazane for silicon dioxide film formation, AIP Adv. 11 (2022) 125328.

[7] S. Yoshimura, S. Sugimoto, T. Takeuchi, M. Kiuchi, Low-energy oxygen ion beam induced chemical vapor deposition using methylsilane or dimethylsilane for the formation of silicon dioxide films, Thin Solid Films 760 (2022) 139508.

[8] S. Yoshimura, S. Sugimoto, T. Takeuchi, K. Murai, M. Kiuchi, Low-energy O^+ ion beam induced chemical vapor deposition using tetraethyl orthosilicate for silicon dioxide film formation, Nucl. Instrum. Method Phys. Res. B 511 (2022) 113-117.

[9] S.Yoshimura, S.Sugimoto, T. Takeuchi, M. Kiuchi, Low-energy Ar+ ion-beam-induced chemical vapor deposition of silicon dioxide films using tetraethyl orthosilicate, Heliyon 9 (2023) e14643 .

[10] Z. Y. Yin, B. K. Garside, Low-loss GeO_2 optical waveguide fabrication using low deposition rate rf sputtering, Appl. Opt. 21 (1982) 4324-4328.

[11] H. Matsubara, T. Sasada, M. Takenaka, S. Takagi, Evidence of low interface trap density in GeO_2/Ge metal-oxide-semiconductor structures fabricated by thermal oxidation, Appl. Phys. Lett. 93 (2008) 032104.

[12] A. Delabie, F. Bellenger, M. Houssa, T. Conard, S. Van Elshocht, M. Caymax, M. Heyns, M. Meuris, Effective electrical passivation of Ge(100) for high-k gate dielectric layers using germanium oxide, Appl. Phys. Lett. 91 (2007) 082904.

[13] S. Chae, L. A. Pressley, H. Paik, J. Gim, D. Werder, B H. Goodge, L. F. Kourkoutis, R. Hovden, T. M. McQueen, E. Kioupakis, J. Heron, Germanium dioxide: A new rutile substrate for epitaxial film growth, J. Vac. Sci. Technol. A 40 (2022) 050401.

[14] T. Ohta, M. Takenaga, N. Akahira, T. Yamashita, Thermal changes of optical properties observed in some suboxide thin films, J. Appl. Phys.53 (1982) 8497-8500.

[15] Y. Takano, Y. Tandoh, H. Ozaki, N. Mori, XPS study on a-GeO_x ($1.3<x<2$) films prepared from GeO_2, Phys. Stat. Sol. 130 (1985) 431-436.

291 [16] J. P. Besse, P. Bondot, P. Fessler, M. Jacquet, Preparation and characterization of
292 germanium oxide thin films, Mat. Res. Bull. 24 (1989) 1361-1367.
293 [17] K. Kita, S. Suzuki, H. Nomura, T. Takahashi, T. Nishimura, A. Toriumi, Direct
294 evidence of GeO volatilization from GeO_2/Ge and impact of its suppression on
295 GeO_2/Ge metal-insulator-semiconductor characteristics, Jpn. J. Appl. Phys. 47
296 (2008) 2349-2353.
297 [18] B. G. Segda, C. Caperaa, M. Jacquet, J. P. Besse, Characterization and dielectric
298 properties of GeOx thin films prepared by radio frequency (RF) reactive sputtering,
299 Nucl. Instrum. Method Phys. Res. B 266 (2008) 4829-4836.
300 [19] A. L. Shabalov, M. S. Feldman, Optical properties of thin GeO_x films, Phys. Stat. Sol.
301 83 (1984) K11-K14.
302 [20] M. Perego, G. Scarel, M. Fanciulli, I. L. Fedushkin, A. A. Skatova, Fabrication of
303 GeO_2 layers using divalent Ge precursor, Appl. Phys. Lett. 90 (2007) 162115.
304 [21] S. Takagi, T. Maeda, N. Taoka, M. Nishizawa, Y. Morita, K. Ikeda, Y. Yamashita, M.
305 Nishikawa, H. Kumagai, R. Nakane, S. Sugihara, N. Sugiyama, Gate dielectric
306 formation and MIS interface characterization on Ge, Microelectr. Eng. 84 (2007)
307 2314-2319.
308 [22] K. N. Astankova, A. S. Kozhukhov, I. A. Azarov, E. B. Gorokhov, D. V. Sheglov,

A. V. Latyshev, Local anodic oxidation of thin GeO films and formation of nanostructures based on them, Phys. Sol. Stat. 60 (2018) 700-704.

[23] D. Kuzum, T. Krishnamohan, A. J. Pethe, A. K. Okyay, Y. Oshima, Y. Sun, J. P. McVittie, P. A. Pianetta, P. C. McIntyre, K. S. Saraswat, Ge-interface engineering with ozone oxidation for low interface-state density, IEEE Electr. Dev. Lett. 29 (2008) 328-330.

[24] Y. Fukuda, T. Ueno, S. Hirano, S. Hashimoto, Electrical characterization of germanium oxide/germanium interface prepared by electron-cyclotron-resonance plasma irradiation, Jpn. J. Appl. Phys. 44 (2005) 6981-6984.

[25] S. Yoshimura, S. Sugimoto, M. Kiuchi, Low-energy mass-selected ion beam production of fragments produced from hexamethyldisilane for SiC film formation, J. Appl. Phys. 119 (2016) 103302.

[26] D. A. Jishiashvili, E. R. Kutelia, Infrared spectroscopic study of GeO_x films, Phys. Stat. Sol. 143 (1987) K147-K150.

[27] T. Matsutani, M. Kiuchi, T. Takeuchi, Preparation of Ge–C films by low-energy ion beam induced chemical vapor deposition with hexamethyldigermane, Nucl. Instrum. Methods Phys. Res. B 257 (2007) 261-264.

[28] S. Yoshimura, S. Sugimoto, T. Takeuchi, K. Murai, M. Kiuchi, Characteristics of

films deposited by the irradiation of $GeCH_x^+$ ions produced from hexamethyldigermane and their dependence on the injected ion energy, Nucl. Instrum. Methods Phys. Res. B 461 (2019) 1-5

[29] J. T. Wang, F. Williams, E.S.R. spectra of the hexamethyldisilane and hexamethyldigermane radical cations, J. Chem. Soc. Chem. Comm. 14 (1981) 666-668.

[30] T. Takeuchi, Y. Shirai, T. Matsutani, M. Kiuchi, Mass spectrometric and theoretical studies on the fragmentation mechanisms of hexamethyldigermane and hexamethyldisilane ions in the gas phase, Nucl. Instrum. Methods Phys. Res. B 232 (2005) 217-222.

[31] S. Yoshimura, S. Sugimoto, T. Takeuchi, M. Kiuchi, Identification of fragment ions produced from hexamethyldigermane and the production of low-energy beam of fragment ion possessing Ge-C bond, AIP Adv. 9 (2019) 025008.

[32] N. Konami, K. Matsuoka, T. Yoshino, S. Matsunaga, Palladium-catalyzed germylation of aryl bromides and aryl triflates using hexamethyldigermane, Synthesis 50 (2018) 2067-2075.

Figure Captions

Fig 1. Schematic drawing of the process chamber of the ion beam system.

Fig 2. The mass spectrum of the ion beam.

Fig 3. The energy spectrum of the O^+-ion beam.

Fig 4. Typical intensity profile for the O^+-ion beam. Horizontal axis represents the distance in the vertical direction.

Fig 5. The dependence of deposited film mass on the O^+-ion energy.

Fig 6. (a) Ge3d, (b) O1s, and (c) C1s X-ray photoelectron spectroscopy spectra of a film deposited following the injection of O^+ ions to a quartz crystal microbalance substrate in conjunction with hexamethyldigermane.

Fig 7. Fourier transform infrared spectrum of a film deposited on a Si substrate following the injection of O^+ ions in conjunction with hexamethyldigermane.

Fig 8. X-ray diffraction pattern (θ-2θ method) of a film deposited on a Si substrate following the injection of O^+ ions in conjunction with hexamethyldigermane.

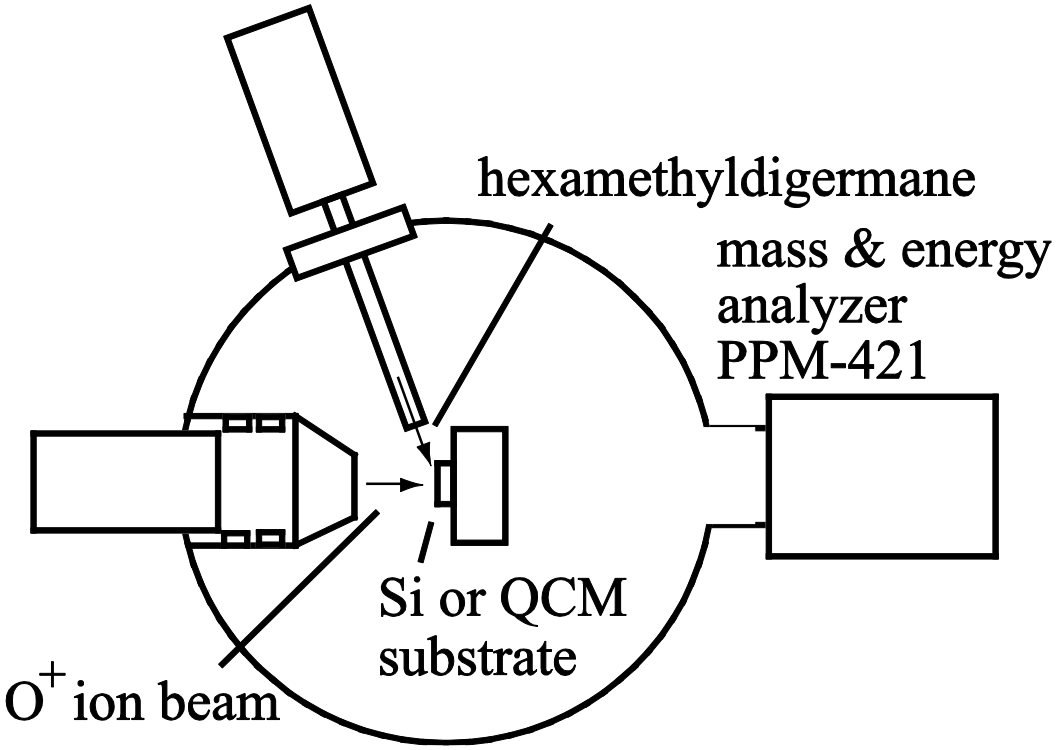

366

367 Fig. 1

368

369

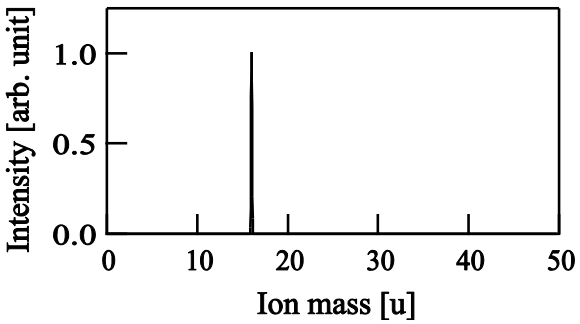

370

371

372 Fig. 2

373

374

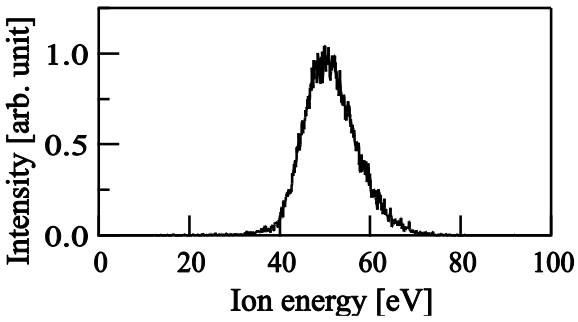

375

376

377 Fig. 3

378

379

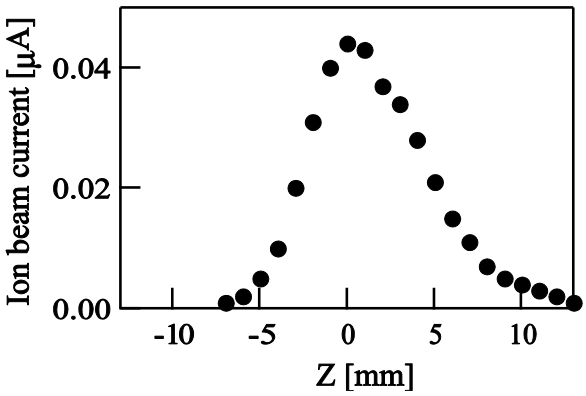

Fig. 4

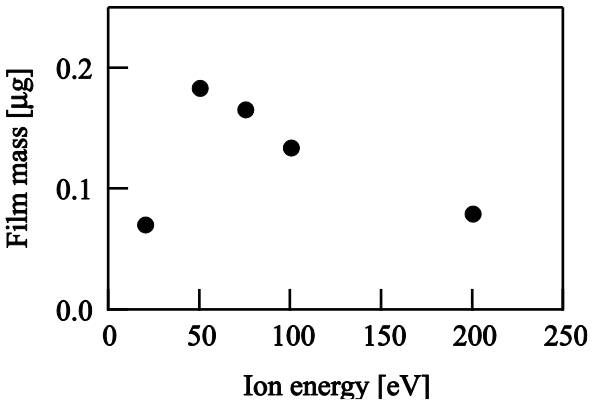

385

386

387 Fig. 5

388

389

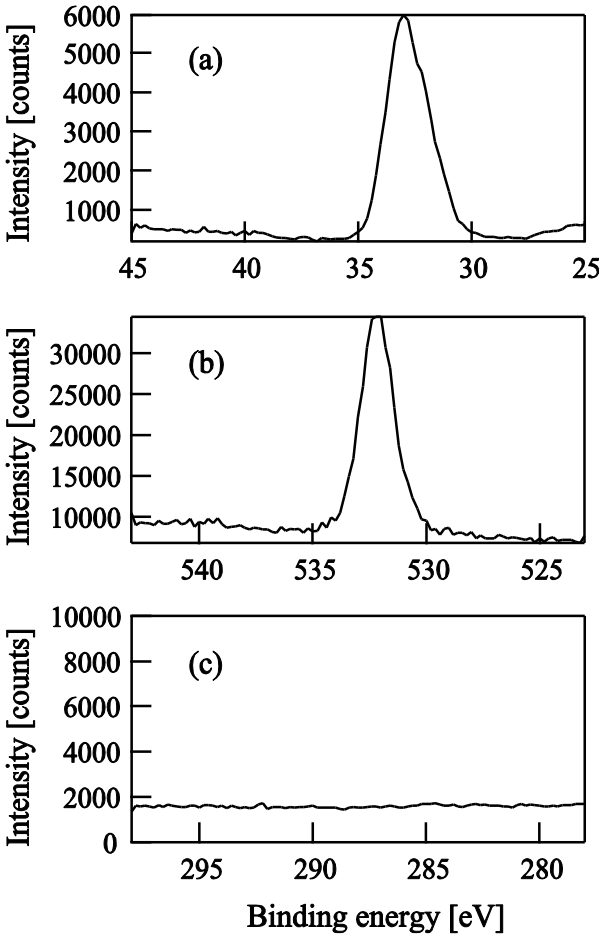
Intensity [counts]
6000
5000
4000
3000
2000
1000
(a)
45
40
35
30
25
Intensity [counts]
30000
25000
20000
15000
10000
(b)
540
535
530
525
Intensity [counts]
10000
8000
6000
4000
2000
0
(c)
295
290
285
280
Binding energy [eV]

Fig. 6

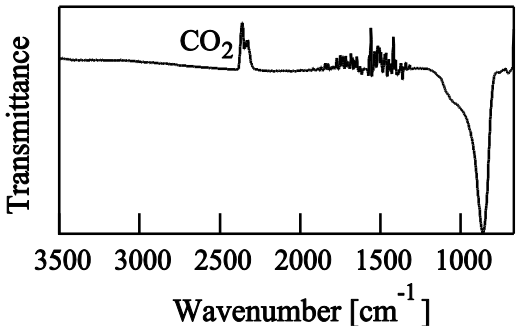

396

397

398 Fig. 7

399

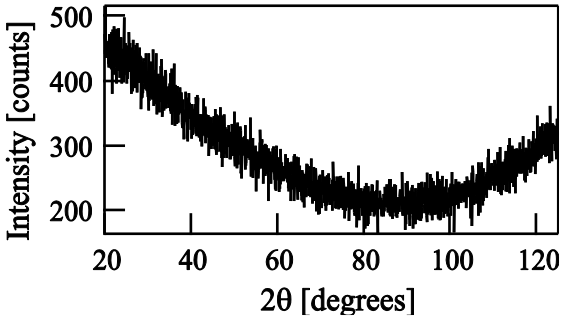

400

401

402 Fig. 8